Catalysis Communications 26 (2012) 218–224

Contents lists available at SciVerse ScienceDirect

Catalysis Communications

journal homepage: www.elsevier.com/locate/catcom

Short Communication

(α-Fe_2O_3)-MCM-41 as a magnetically recoverable nanocatalyst for the synthesis of pyrazolo[4,3-c]pyridines at room temperature

Shahnaz Rostamizadeh *, Nasrin Shadjou, Mohammad Azad, Nima Jalali

Department of Chemistry, K. N. Toosi University of Technology, P.O. Box 15875-4416, Tehran, Iran

ARTICLE INFO

Article history:
Received 23 April 2012
Received in revised form 24 May 2012
Accepted 28 May 2012
Available online 2 June 2012

Keywords:
Pyrazolo[4,3-c]pyridines
Magnetically separable catalyst
(α-Fe_2O_3)-MCM-41

ABSTRACT

MCM-41 embedded magnetic nanoparticles which was prepared through the formation of MCM-41 in the presence of Fe_3O_4 nanoparticles has been used as a magnetically recoverable catalyst for the synthesis of new series of pyrazolo[3,4-c]pyridine derivatives. This catalyst with 10 wt.% of loaded iron oxide nanoparticles was highly recyclable (up to 5 times), and was easily recovered from the reaction mixture using an external magnet without loss of activity. The prepared magnetic catalyst is characterized by X-ray powder diffraction (XRD), transmission electron microscopy (TEM), Fourier transform infrared (FT-IR), nitrogen physisorption measurements, and acid–base titration.

1. Introduction

The magnetic iron oxide nanoparticles are particularly attractive owing to their unique properties and potential applications in various fields, such as magnetically assisted drug delivery, magnetic resonance imaging (MRI) contrast agents, hyperthermia, and magnetic separation of biomolecules [1–3]. In general, the naked nanoparticles always tend to aggregate into large clusters and thus lose their specific properties. This problem can be overcome by coating the nanoparticles with silica, polymer or carbon shells [4–6].

Since the first discovery in 1992, mesoporous molecular sieves have attracted significant attention in the field of adsorption, catalysis, and separation as they exhibit excellent characteristics such as a high surface area up to 1500 $m^2\,g^{-1}$, a large pore volume, and a narrow pore size distribution between 2 and 15 nm [7–10]. MCM-41 (Mobil Composition of Matter No. 41)—as a highly ordered mesoporous material—was used as one of the best neutral coating layers to confine magnetic nanoparticles, due to its high chemical and thermal stability, large surface area and good compatibility [11].

The integration of mesoporous silica with magnetic nanoparticles to form porous magnetic nanocomposite is undoubtedly of great interest for practical applications. This type of magnetic nanocomposites, have the advantages of both mesoporous silica and magnetic nanoparticles.

Magnetic separation provides a convenient method for removing and recycling magnetized species by applying an appropriate magnetic field. Up to now, several papers have reported the synthesis and application of these magnetic nanocomposites in organic manufacturing [12].

The pyrazolo[4,3-c]pyridine ring system is present in numerous biologically active natural products as well as many synthetic compounds. They are important heterocyclic compounds, which exhibit a diverse range of biological properties such as inhibitors of xanthine oxidases, and as compounds for the inhibition of cholesterol formation [13]. A new series of these types of compounds also exhibit a modest CNS depressant and anti-inflammatory activity [14].

In view of these useful properties, an efficient and general method for the synthesis of these compounds and their derivatives has not been reported yet. But microwave heating in the solid state [15], and refluxing α,β-unsaturated ketones with hydrazine hydrate in ethanol and methanol for 10 h in the presence of Na are the only previously reported methods [16]. However, these methods are time-consuming

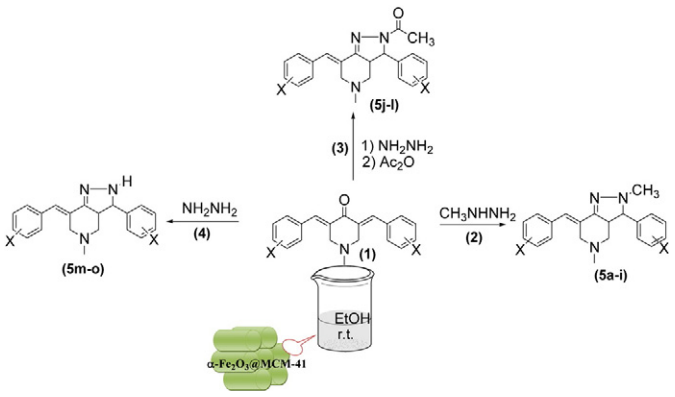

Scheme 1. Synthesis of pyrazolo[4,3-c]pyridine derivatives in the presence of (α-Fe_2O_3)–MCM-41.

* Corresponding author. Fax: +98 21 22853650.
E-mail address: rostamizadeh@kntu.ac.ir (S. Rostamizadeh).

1566-7367/$ – see front matter © 2012 Elsevier B.V. All rights reserved.
doi:10.1016/j.catcom.2012.05.022

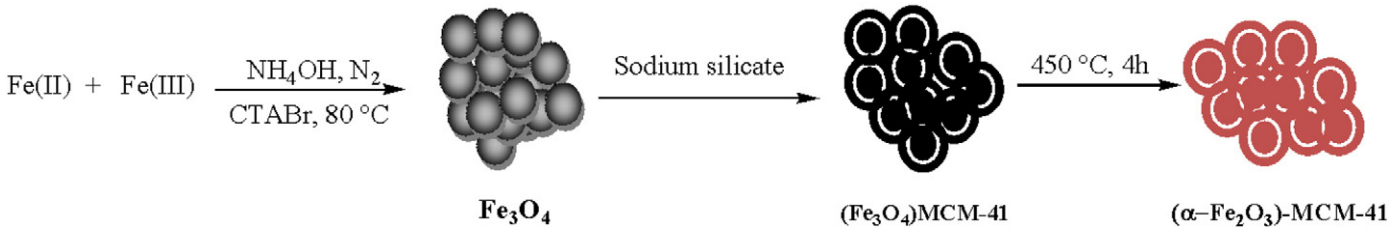

Scheme 2. Preparation of (α-Fe_2O_3)–MCM-41 nanocatalyst.

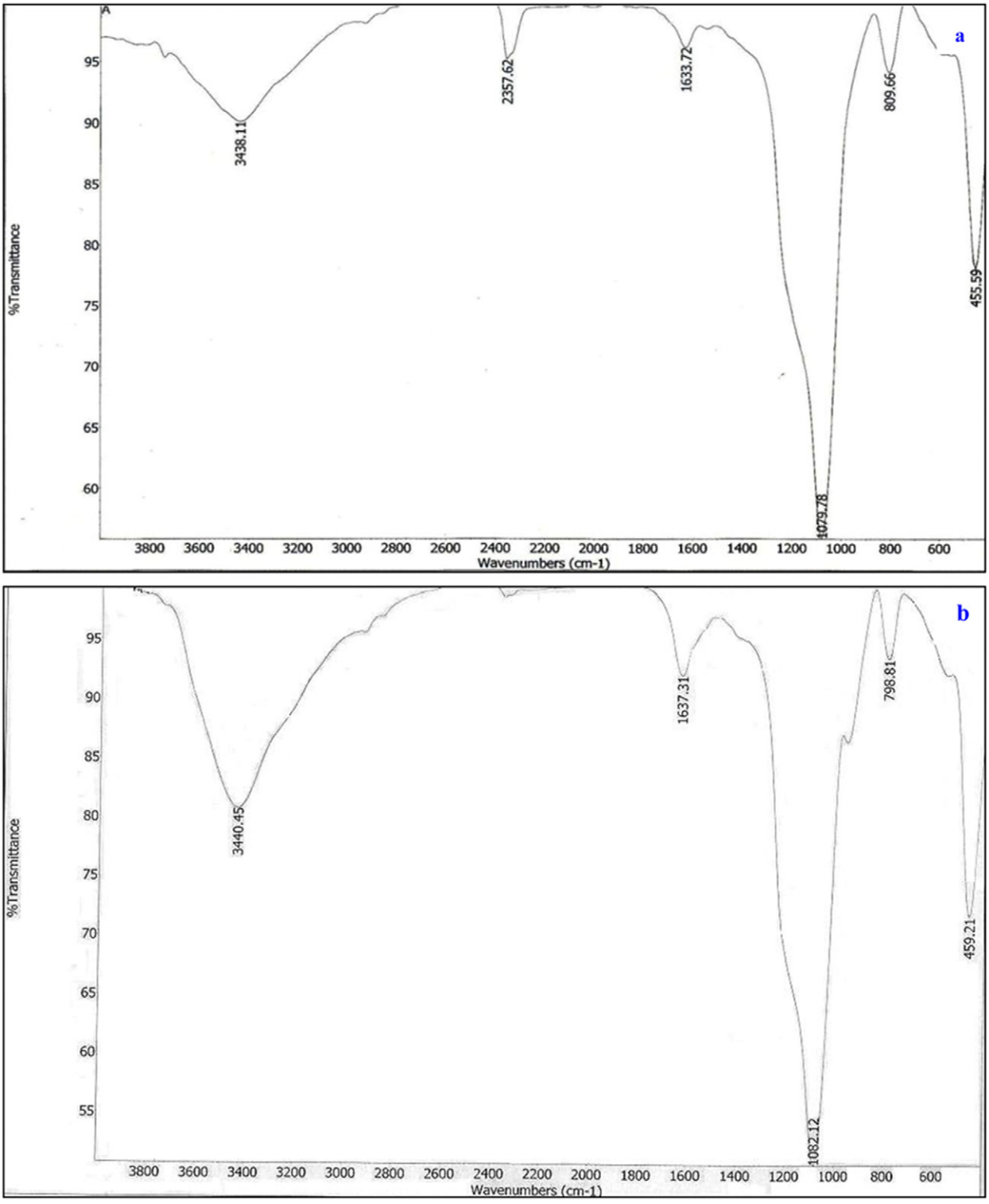

Fig. 1. The IR spectra of a) as prepared and b) recovered (α-Fe_2O_3)–MCM-41.

and use toxic solvents and reagents. Thus, the development of a green, simple, efficient, and general method for the synthesis of these widely used organic compounds from readily available reagents remains one of the major challenges in organic synthesis.

In connection with our interest in the preparation and use of solid catalysts for the production of fine chemicals [17], and because of the inherent properties like environmental friendliness, greater selectivity, operational simplicity, non-corrosive nature, moisture insensitivity, and ease of isolation, it is of interest to determine the behavior of this catalytic system (α-Fe_2O_3)–MCM-41) for the synthesis of pyrazolo[4,3-c]pyridine derivatives from the reaction of α,β-unsaturated ketones with hydrazine hydrate, methyl hydrazine, and hydrazine hydrate together with acetic anhydride in ethanol at room temperature (Scheme 1).

2. Experimental

2.1. Preparation of the catalyst

A solution with molar composition of 3.2 $FeCl_3$:1.6 $FeCl_2$:1 CTABr:39 NH_4OH: 2300 H_2O was used for preparation of naked Fe_3O_4 nanoparticles at room temperature. Typically, 2 g of iron (III) chloride ($FeCl_3.6H_2O$) and 0.8 g of iron (II) chloride ($FeCl_2{\cdot}4H_2O$) were dissolved in 10 mL of distilled water under N_2 atmosphere. The resultant solution dropwisely was added to a 100 mL solution of 1.0 M NH_4OH containing 0.4 g of cetyltrimethylammonium bromide (CTABr) to construct a colloidal suspension of iron oxide magnetic nanoparticles. The magnetic MCM-41 was prepared by adding 20 mL of the magnetic colloid to a 1 L solution with the molar composition of 292 NH_4OH:1 CTABr: 2773 H_2O under vigorous mixing and sonication. Then sodium silicate (16 mL) was added, and the mixture was allowed to react at room temperature for 24 h under stirring. The magnetic MCM-41 was filtered and washed. The surfactant template was then removed from the synthesized material by calcination at 450 °C for 4 h and the (Fe_3O_4)–MCM-41 converted to (α-Fe_2O_3)–MCM-41. It is worth mentioning that in the absence of nitrogen the magnetic property of Fe_3O_4 is decreased.

3. Results and discussion

At first the (α-Fe_2O_3)–MCM-41 with 10 wt.% of loaded iron oxide nanoparticles was prepared according to the method reported in literature with some modifications (Scheme 2) [18].

The prepared and recovered catalyst was characterized with IR spectra. In IR spectra, the band from 400–650 cm^{-1} is assigned to the stretching vibrations of (Fe – O) bond in α-Fe_2O_3, and the band at about 1100 cm^{-1} is belong to the stretching of the (Si – O) bond (Fig. 1).

The XRD analysis of was performed from 1.0° (2θ) to 10.0° (2θ). The sample of (α-Fe_2O_3)–MCM-41 showed relatively well-defined XRD patterns, with one major peak along with two small peaks identical to those of MCM-41 materials (Fig. 2a). In addition, XRD pattern in the region of 10.0° (2θ) to 80.0° (2θ) confirmed that change of sample's color from black to brick-red after calcination of the catalyst is due to the oxidation of embedded Fe_3O_4 to α-Fe_2O_3 nanoparticles (Fig. 2b) [19].

Also the XRD analysis of recovered catalyst was recorded in the region of 2.0° (2θ) to 80.0° (2θ) in which the position and relative intensities of all peaks was confirmed well with the XRD pattern of as prepared catalyst and no leaching of embedded nanoparticles was observed (Fig. 3).

TEM micrograph of prepared catalyst (Fig. 4c) shows an ordered hexagonal pore system with embedded α-Fe_2O_3 nanoparticles. Also uniform and spherical morphology of the catalyst was confirmed by SEM images (Fig. 4a, b).

The specific surface area and pore volume obtained by the N_2 adsorption isotherms and calculated by the Brunauer–Emmett–Teller

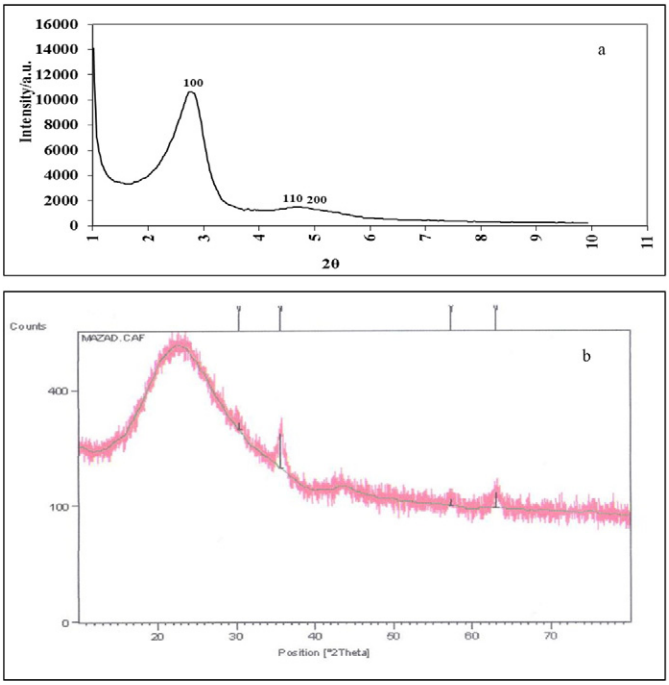

Fig. 2. XRD patterns of the (α-Fe_2O_3)–MCM-41 in the region of (2θ) equal to a) 1.0° to 10.0° (2θ) and b) 10.0° to 80.0°.

(BET) method [20] were 1213 $m^2\ g^{-1}$ and 1.59 $cm^3\ g^{-1}$ respectively. The pore diameter of the (α-Fe_2O_3)–MCM-41 was 5.26 nm derived from the adsorption and desorption branches by the Broekhoff and deBoer model (Fig. 5) [21].

In addition surface acidity of the catalyst was determined with acid–base titration and it was found that the catalyst has not considerable acidic property.

During optimization of the reaction conditions, at first we chose 3,5-bis(4-chlorobenzylidene)-1-methylpiperidin-4-one (0.16 mmol) and hydrazine hydrate (0.16 mmol) in ethanol as model reactants and examined the effect of the amount of the catalyst. According to these data, the optimum amount of catalyst was 0.015 g. Increasing the amount of catalyst did not improve the yield and the reaction time, while in the absence of the catalyst the low yield of product was achieved (Table 1 entries 1–3). It should be mentioned that in the presence of pure MCM-41, amino-functionalized MCM-41 (MCM-41–$nPrNH_2$) and Fe_3O_4 nanoparticles (Table 1 entries 4–6) the time and

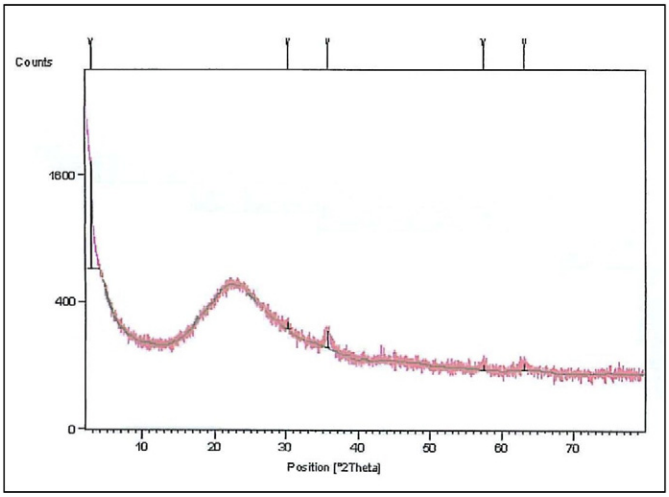

Fig. 3. The XRD patterns of recovered catalyst in the region of 2.0° to 80.0° (2θ).

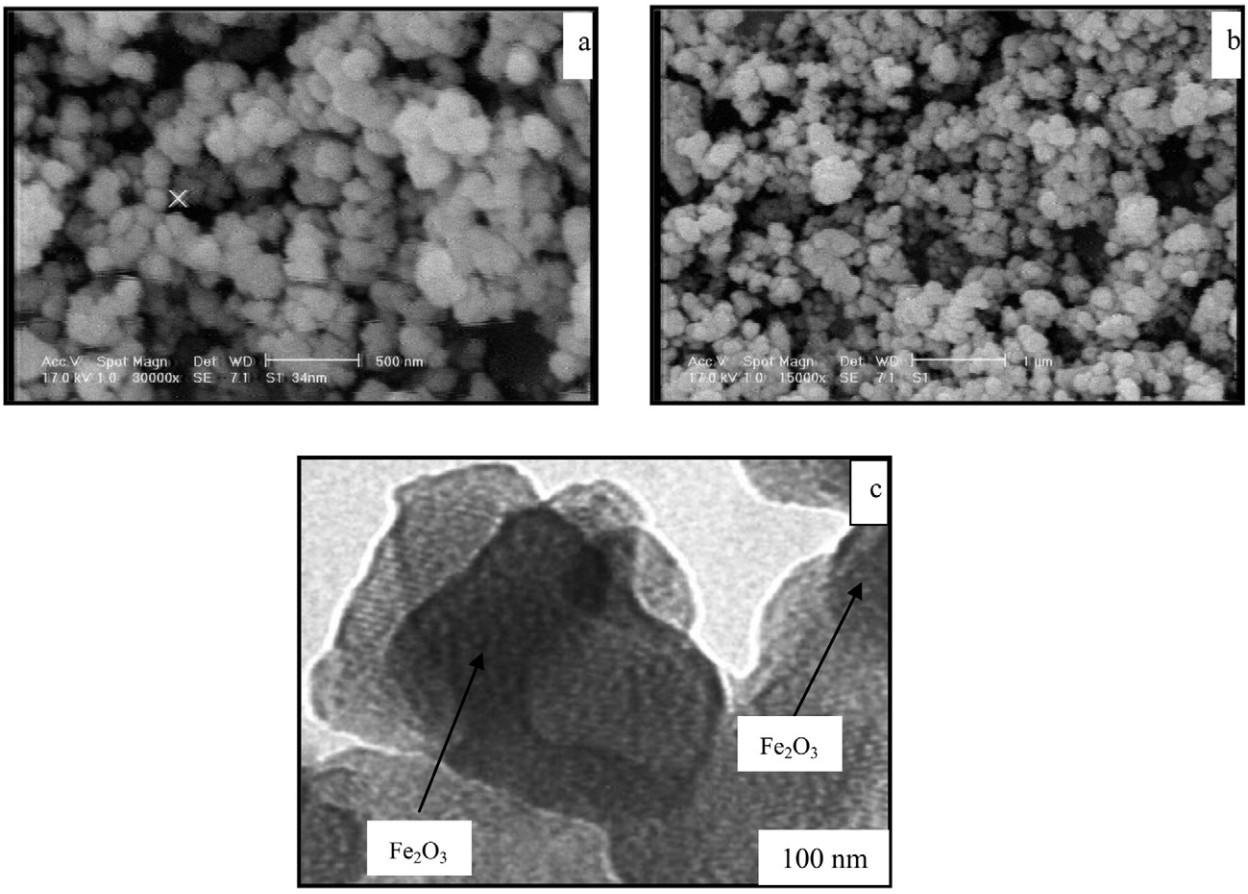

Fig. 4. The SEM (a, b) and TEM (c) images of (α-Fe_2O_3)–MCM-41.

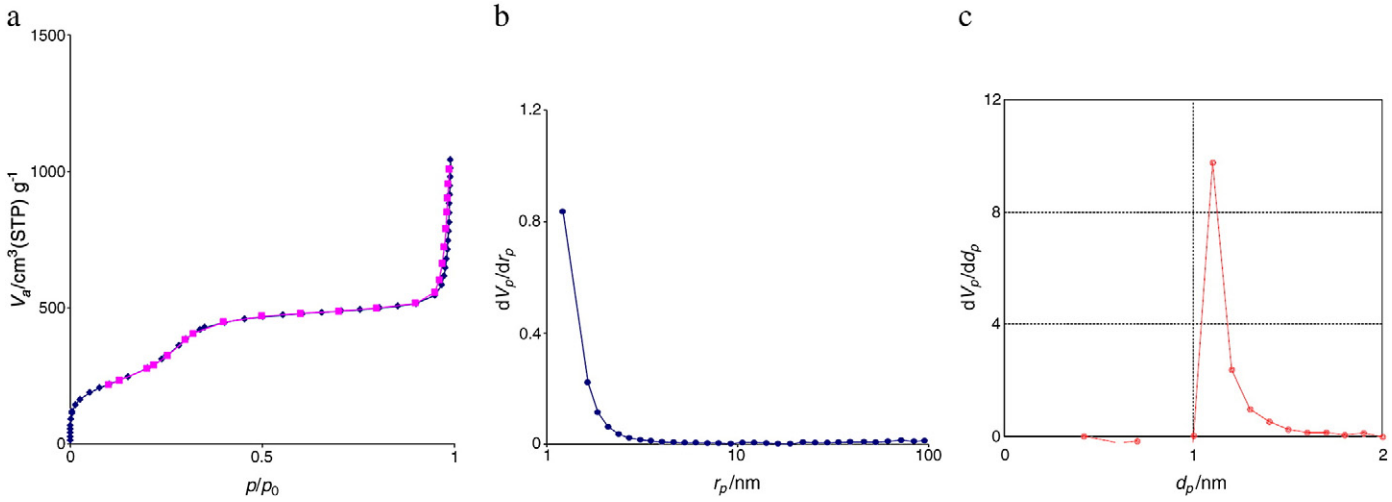

Fig. 5. (a) Nitrogen adsorption/desorption isotherm, (b) BJH and (c) Pore size distribution of (α-Fe_2O_3)–MCM-41.

Table 1
Comparison of the amount of the catalyst and yields for the synthesis of **5j**.

Entry	Catalyst	Amount of the catalyst (g)	Time (min)	Yield (%)
1	–	–	>240	40
2	(α-Fe_2O_3)–MCM-41	0.015	20	96
3	(α-Fe_2O_3)–MCM-41	0.02	20	97
4	Pure MCM-41	0.015	60	85
5	MCM-41–$nPrNH_2$	0.015	40	92
6	Fe_3O_4 nanoparticles	0.015	30	95

Table 2
Solvent screening for the synthesis of **5j** in the present of 0.015 g of (α-Fe_2O_3)–MCM-41.

Entry	Solvent	Time (min)	Yield (%)
1	CH_3CN	60	70
2	CH_3OH	25	95
3	C_2H_5OH	20	96
4	H_2O	180	No reaction

Table 3
The reaction time (min) and the yield (%) of pyrazolo[4,3-c]pyridine product.

Entry	Product	Time (min)	Yield* (%)	M.P (°C) Found	M.P (°C) Reported
5a	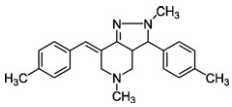	30	97	143–144	118–120 [16]
5b	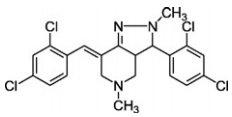	15	98	212–214	–
5c	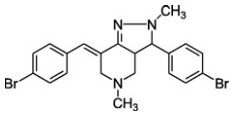	15	90	160–161	–
5d	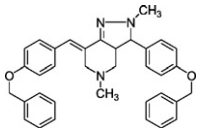	30	95	166–167	–
5e	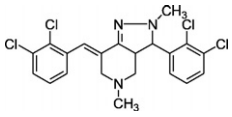	15	98	205	–
5f	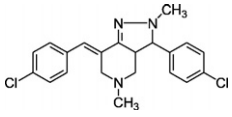	15	98	148–149	–
5g	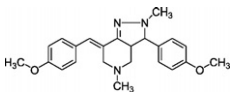	20	90	183–184	182–183 [16]
5h	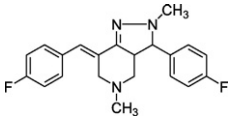	10	98	121–123	–
5i	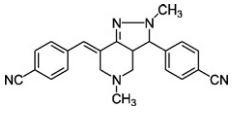	10	98	207–208	–
5j	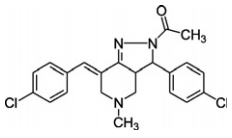	20	96	156–157	–
5k	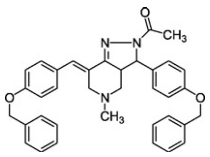	>60	90	189–190	–
5l	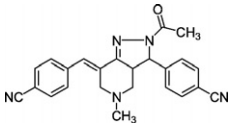	30	95	255–256	–

Table 3 (*continued*)

Entry	Product	Time (min)	Yield* (%)	M.P (°C) Found	M.P (°C) Reported
5m	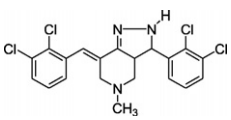	40	95	130–132	–
5n	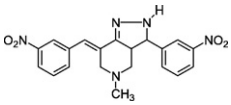	30	96	149–150	–
5o	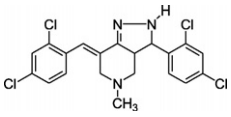	45	98	186–189	–

the yield of the reaction was satisfactory, but because of the ease of recovery and reusability of (α-Fe_2O_3)–MCM-41, this catalyst was therefore chosen (Table 1).

To check the effect of solvents the model reaction was separately performed in different solvents such as CH_3CN, CH_3OH, C_2H_5OH, and H_2O in the present of 0.015 g of catalyst from which C_2H_5OH was found to be the best (Table 2).

With these results in hand, a variety of aromatic aldehydes, possessing both electron-donating and electron-withdrawing groups were employed for pyrazolo[4,3-c]pyridine formation and the results indicated that for 3,5-dibenzylidenepiperidin-4-one bearing different functional groups, the reaction proceeded smoothly in all cases. It is worth mentioning that 3,5-dibenzylidenepiperidin-4-one with electron-withdrawing groups on the phenyl rings induce greater electronic positive charge on the corresponding β-atoms and reacted rapidly whereas electron-rich groups on the phenyl rings require longer reaction times. Also N-acetyldihydropyrazoles (**5j**–**5l**) were also synthesized by addition of hydrazine hydrate to 3,5-dibenzylidenepiperidin-4-one (**1**) and subsequent acylation of bicyclic compounds with acetic anhydride. Among the six derivatives of 3,5-dibenzylidenepiperidin-4-one (4-chloro, 4-benzyloxy, 4-cyano, 2,3-dichloro, 3-nitro, 2,4-dichloro) that have been used, only 4-chloro, 4-benzyloxy and 4-cyano reacted with hydrazine and then acylated with acetic anhydride (Table 3).

A plausible mechanism for the formation of pyrazolo[4,3-c] pyridines is shown in Scheme 3. Because of the Lewis acidity property

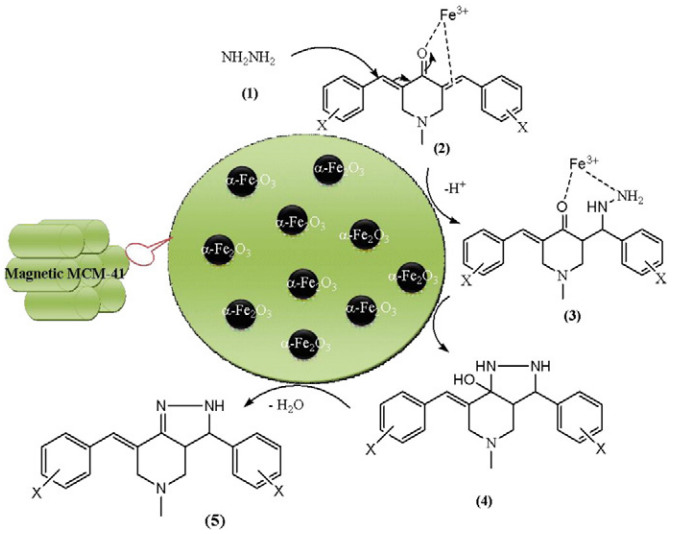

Scheme 3. A proposed mechanism for the synthesis of pyrazolo[4,3-c]pyridines.

Table 4
Other reported methods for the synthesis of pyrazolo[4,3-c]pyridines.

Product	Reaction condition/Solvent	Time (h)	Yield (%)
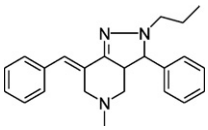	Reflux/MeOH	0.5–7	53 [22]
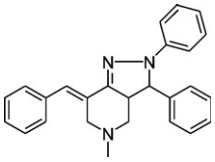	Reflux/EtOH	6	72 [23]
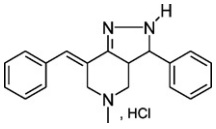	Reflux/MeOH	4	78 [14]
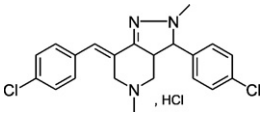	Reflux/MeOH	4	80 [14]
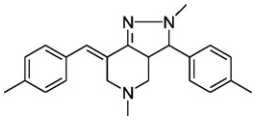	Reflux/EtOH	10	28 [16]
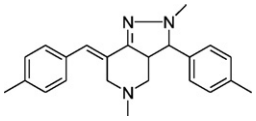	Room temperature/EtOH	1/2	97

of the Fe^{3+}, the intermediate (**3**) can be formed through the reaction of hydrazine hydrate (**1**) with activated C═C double bond of 3,5-dibenzylidenepiperidin-4-one (**2**). Then, the nucleophilic attack of the other NH_2 group on the carbonyl (C═O) moiety gives intermediate (**4**). Finally, the expected product (**5**) is afforded by water elimination.

Also, our synthetic method has been compared with other methods reported in the literature (Table 4). As can be seen, most of them have been synthesized at high temperature or reflux conditions. By using the (α-Fe_2O_3)–MCM-41 as catalyst, the reaction has been done at room temperature without any need to heating or refluxing.

It is important to note that the magnetic property of this catalyst facilitates its efficient recovery from the reaction mixture during work-up procedure. In the presence of an external magnet, recoverable (α-Fe_2O_3)–MCM-41 moved onto the magnet steadily and the reaction mixture turned clear within 10 s. Thus, the catalyst effectively collected and the recovered catalyst was used in subsequent runs without observation of significant decrease in activity even after 5 runs (Fig. 6).

4. Conclusion

In summary, (α-Fe_2O_3)–MCM-41 was found to be a new, efficient and magnetically recyclable catalyst for the synthesis of a variety of pyrazolo[4,3-c]pyridine derivatives. The catalyst was separated with an external magnet, and was used in subsequent runs without observation of significant decrease in activity even after 5 runs. Recovery and reusability of the catalyst, good to high yields, short reaction times, simple work-up, and the ecologically clean procedure make this method attractive and useful.

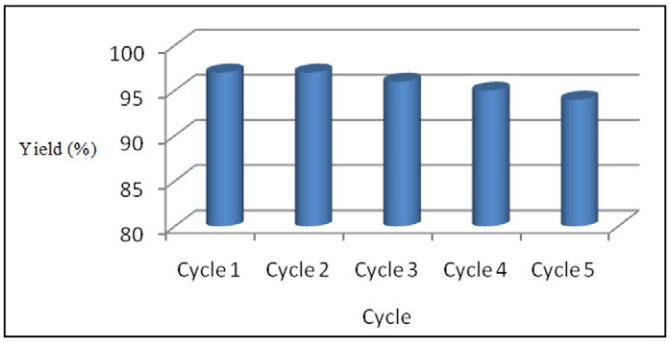

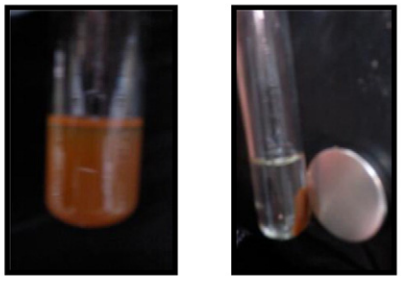

Fig. 6. Catalyst recovery at the end of the reaction.

Acknowledgments

Authors gratefully acknowledge the Research Council of K. N. Toosi University of Technology for partial financial support of this work.

Appendix A. Supplementary data

Supplementary data to this article can be found online at http://dx.doi.org/10.1016/j.catcom.2012.05.022.

References

[1] J.A. Melero, R.V. Grieken, G. Morales, Chemical Reviews 106 (2006) 3790.
[2] D. Astruc, F. Lu, J.R. Aranzaes, Angewandte Chemie International Edition 44 (2005) 7852.
[3] S. Morent, S. Vasseur, F. Grasset, E. Duguet, Journal of Materials Chemistry 14 (2004) 2161.
[4] H. Yoon, S. Ko, J. Jang, Chemical Communications (2007) 1468.
[5] E. Ye, B.H. Liu, W.Y. Fan, Chemistry of Materials 19 (2007) 3845.
[6] B.J. López, C. Boissière, C. Chanéac, D. Grosso, S. Vasseur, S. Miraux, E. Duguet, C. Sanchez, Journal of Materials Chemistry 17 (2007) 1563.
[7] D. Zhao, Q. Huo, J. Feng, B.F. Chmelka, G.D. Stucky, Journal of the American Chemical Society 120 (1998) 6024.
[8] W. Zhang, T.R. Pauly, T.J. Pinnavaia, Chemistry of Materials 9 (1997) 2491.
[9] A. Galarneau, D. Desplantier-Giscard, F. Di Renzo, F. Fajula, Catalysis Today 68 (2001) 191.
[10] F. Hoffmann, M. Cornelius, J. Morell, M. Fröba, Angewandte Chemie International Edition 45 (2006) 3216.
[11] Z.Y. Lu, J. Dai, X.N. Song, G. Wang, W.S. Yang, Colloids and Surfaces A 317 (2008) 450.
[12] (a) L. Ma'mani, A. Heydari, M. Sheykhan, Applied Catalysis A: General 384 (2010) 122; (b) Y.H. Liu, J. Deng, J.W. Gao, Z.H. Zhang, Advanced Synthesis and Catalysis 354 (2012) 441.
[13] Y. Fujikawa, M. Suzuki, H. Iwasaki, M. Sakashita, M. Kitahara, European Patent Application EP 339 (1989) 358.
[14] J. Krapcho, C.F. Turk, Journal of Medicinal Chemistry 22 (1979) 207.
[15] J.-H. Peng, W.-J. Hao, S.-J. Tu, Journal of Heterocyclic Chemistry 46 (2009) 849.
[16] H.I. El-Subbagh, S.M. Abu-Zaid, M.A. Mahran, F.A. Badria, A.M. Al-Obaid, Journal of Medicinal Chemistry 43 (2000) 2915.
[17] (a) S. Rostamizadeh, A.M. Amani, G.H. Mahdavinia, G. Amiri, H. Sepehrian, Ultrasonics Sonochemistry 17 (2010) 306; (b) S. Rostamizadeh, A.M. Amani, G.H. Mahdavinia, H. Sepehrian, S. Ebrahimia, Synthesis (2009) 1356;

(c) S. Rostamizadeh, A. Amirahmadi, N. Shadjou, A.M. Amani, Journal of Heterocyclic Chemistry 49 (2012) 111.
[18] X. Chen, K.F. Lam, Q. Zhang, B. Pan, M. Arruebo, K.L. Yeung, Journal of Physical Chemistry C 113 (2009) 9804.
[19] V.R. Elías, M.I. Oliva, E.G. Vaschetto, S.E. Urreta, G.A. Eimer, S.P. Silvetti, Journal of Magnetism and Magnetic Materials 322 (2010) 3438.
[20] H. Takahashi, B. Li, T. Sasaki, C. Miyazaki, T. Kajino, S. Inagaki, Microporous and Mesoporous Materials 44–45 (2001) 755.
[21] E.P. Barrett, L.G. Joyner, P.H. Halenda, Journal of the American Chemical Society 73 (1951) 373.
[22] G.C. Rovnyak, R.C. Millonig, J. Schwartz, V. Shu, Journal of Medicinal Chemistry 25 (1982) 1482.
[23] N.V. Sviridenkova, S.Z. Vatsadze, M.A. Manaenkova, N.V. Zyk, Russian Chemical Bulletin 54 (2005) 2590.